Manuscript Submission

Accident Analysis & Prevention

A video-based assessment of cyclist-tram track interactions in wet road conditions

Submitted: Sunday 23rd October, 2022

A video-based assessment of cyclist-tram track interactions in wet road conditions*

Kevin Gildea[1], Daniel Hall[1], Clara Mercadal-Baudart[1], Brian Caulfield[2], and Ciaran Simms[1]

[1]Department of Mechanical, Manufacturing & Biomedical Engineering, Trinity College Dublin
[2]Department of Civil, Structural & Environmental Engineering, Trinity College Dublin

Submitted: October 23rd, 2022

Abstract

Single cyclist/bicycle collisions are common and underreported in official statistics. In urban environments, light rail tram tracks are a frequent factor, however, they have not yet been the subject of engineering analysis. The prevalence of traffic camera footage in urban environments presents an opportunity for detailed site-specific safety insights.

In this study, we present a video-based frequency and risk analysis for unsuccessful crossings on tram tracks in wet road conditions at 9 locations around Dublin city centre, Ireland. We also devise a predictive model for crossing success as a function of crossing angle for use in a surrogate safety measure framework.

Modelling results show that crossing angle is a strong predictor of crossing success, and that cyclist velocity is not. Findings indicate that infrastructural planners should design for cyclist crossing angles of 30°or greater. We highlight the prevalence of external factors which limit crossing angles for cyclists. In particular, kerbs are a common factor, along with passing/approaching vehicles or other cyclists. Furthermore, we introduce a new Surrogate Measure of Safety (SMoS) for cyclist interactions with tram tracks, and demonstrate its utility with an open-source application (SafeCross), which is available through the project page.

Keywords— Single cyclist collisions, Single bicycle crashes, Tram tracks, Video analysis, Risk modelling, Surrogate Measures of Safety, Computer vision, Cyclist detection

*Draft manuscript. Please do not share without the authors' permission.

1 Introduction

Findings from (Gildea and Simms 2021) show that single cyclist collisions are unlikely to appear in police statistics. Specifically, the odds of cyclist-motorised vehicle collisions being reported to the police in Ireland are estimated to be 20 times greater than in Ireland, similar to international estimates (Shinar, Valero-Mora, van Strijp-Houtenbos, Haworth, Schramm, De Bruyne, Cavallo, Chliaoutakis, Dias, Ferraro, Fyhri, Sajatovic, Kuklane, Ledesma, Mascarell, Morandi, Muser, Otte, Papadakaki, Sanmartín, Dulf, Saplioglu, and Tzamalouka 2018). This bias leads to an underestimation of their importance among researchers and policymakers (Schepers, de Geus, van Cauwenberg, Ampe, and Engbers 2020). For this reason, while collision/injury prevention strategies for collisions with vehicles are well-investigated, strategies for mitigating single cyclist collisions are not.

Common cyclist collision configurations and contributory factors for single cyclist collisions are investigated in (Gildea, Hall, and Simms 2021). Findings indicate that falls involving interactions with light rail tram tracks are common in the city of Dublin. Tram tracks were the most common infrastructural collision partner, and a contributing factor in 23% of single cyclist collisions (ibid.). Internationally, other self-reporting studies also highlight their importance, with 19% of cases in a study in Melbourne (Beck, Stevenson, Cameron, Oxley, Newstead, Olivier, Boufous, and Gabbe 2019), and 13% of cases in a study in Switzerland (Hertach, Uhr, Niemann, and Cavegn 2018) involving tram tracks.

A previous video analysis of cyclists crossing railway tracks found that the minimum safe approach angle for crossing railway tracks is 30° (Ling, Cherry, and Dhakal 2017), however, this study relied on visual assessments of crossing angles (10° bins), and it is unclear whether these findings also translate to light-rail tracks where there are frequent interactions with cyclists in crowded urban environments. Along with increasing popularity of cycling, many new light rail

systems are being implemented across Europe as part of a broader move towards sustainable transport (UITP 2019). Accordingly, further investigation is required to understand potential conflicts.

As detailed data on crossing angles are not routinely captured in police, hospital, or insurance databases, and given the prevalence of traffic cameras along tram systems, video-based approaches have obvious potential for these cases. Traffic camera footage is often used for analysis of collisions (Johnson, Charlton, Oxley, and Newstead 2010; Ling, Cherry, and Dhakal 2017), as well as near-collision or near-miss incidents and Surrogate Measures of Safety (SMoS) or Surrogate Safety Measures (SSM), i.e., a safety-related indicator without the need for collision footage, allowing for rapid proactive assessment of potential areas of conflict. This approach is potentially more cost-effective than analysis of historic crash data analysis, and is well aligned with the proactive element of Safe System approach to road safety. A variety of SMoS metrics exist, e.g. Time To Collision (TTC) (Hayward 1971), Post-Encroachment Time (PET) (Allen, Shin, and Cooper 1978), or bicycle Deceleration Rate (DR) (Strauss, Zangenehpour, Miranda-Moreno, and Saunier 2017). Generally, these metrics are based on vehicle trajectories (direction, velocity, acceleration), and sometimes mass (Extended Delta-V) (Laureshyn, de Goede, Saunier, and Fyhri 2017), which are used as proxies for collision risk. Various open-source software exist for SMoS analysis with traffic camera footage, e.g., T-analyst[1], Traffic Intelligence project[2], and Surveillance Tracking Using Deep Learning (STRUDL)[3]. After collection of traffic camera footage, a common first step is camera calibration to determine the relationship between pixel coordinates and the ground-plane, after which road user tracking is performed. Tracking may be manual (e.g., T-analyst), or automatic (e.g., STRUDL (Bornø Jensen, Ahrnbom, Kruithof, Åström, Nilsson, Ardö, Laureshyn, Johnsson, and Moeslund 2019)), i.e., using deep neural networks.

[1] https://bitbucket.org/TrafficAndRoads/tanalyst/wiki/Home/
[2] https://bitbucket.org/Nicolas/trafficintelligence/wiki/Home/
[3] https://github.com/ahrnbom/strudl/

2 Study aims

Therefore, this study aims to use traffic camera footage to identify site-specific safety issues between cyclists and tram tracks, correlate unsuccessful crossing risk with crossing trajectories, and devise a validated SMoS algorithm for future use in safety assessments.

3 Methods

3.1 Data collection

Traffic camera footage was collected in October/November 2021 following ethical approval from the School of Engineering, Trinity College Dublin. This involved manual screening, annotation and extraction of cyclist interactions with tram tracks from 9 locations (10 cameras) in Dublin city centre (Figure 1). Locations with an established likelihood of cyclist-tram track conflicts were chosen based on findings from (Gildea, Hall, and Simms 2021), and feedback from experts in the city council. The analysis focuses on weekdays, daylight conditions, and peak commuting hours (Gildea and Simms 2021). Initially, a sample that included both dry and wet conditions was assessed, but a preliminary analysis found no falls during dry conditions. Wet road conditions are a significant factor for cyclist falls on tracks (Gildea, Hall, and Simms 2021; Ling, Cherry, and Dhakal 2017). Therefore, the final analysis focused on periods with wet road conditions.

3.2 Track description and effective groove gap width

Various light rail track profiles exist. The popular girder grooved rail types are limited to the European standards: Ri 59N, Ri 60N, IC, Ri52N, Ri53N, NP4a, and 35G. Rail heads are similar

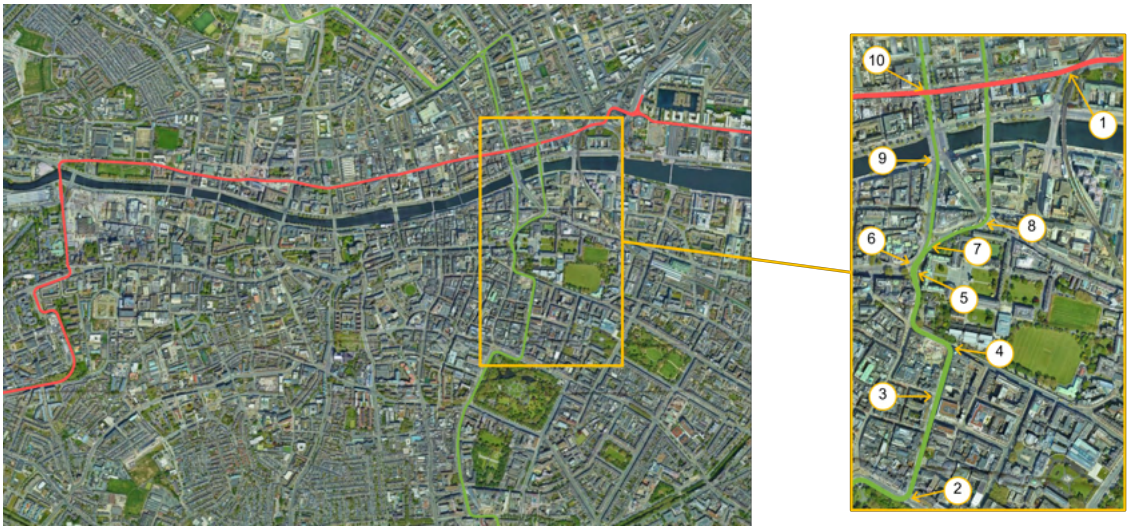

Figure 1: Study locations in Dublin city centre.

across all types, however, the width of the groove gap differs. The Irish tram service (Luas) uses the Ri59N (Ri 59-R13) girder grooved rail in shared-space environments, i.e., most street-running sections and stops (Figure 18). Pavement/asphalt is set around the rail to support the shared use of the road.

Larger groove gap widths present larger risks to crossing cyclists, and this is exacerbated by off-perpendicular crossing angles (<90°). This increased risk can be expressed in the form of an effective width of the groove gap (EW) when crossing at an angle (θ) (Skelton 2016). The relationship between θ and EW is plotted for various track types in Figure 2, showing EW tends to infinity as angle approaches 0°. Furthermore, as crossing angle reduces the differences between effective widths of the track types widens.

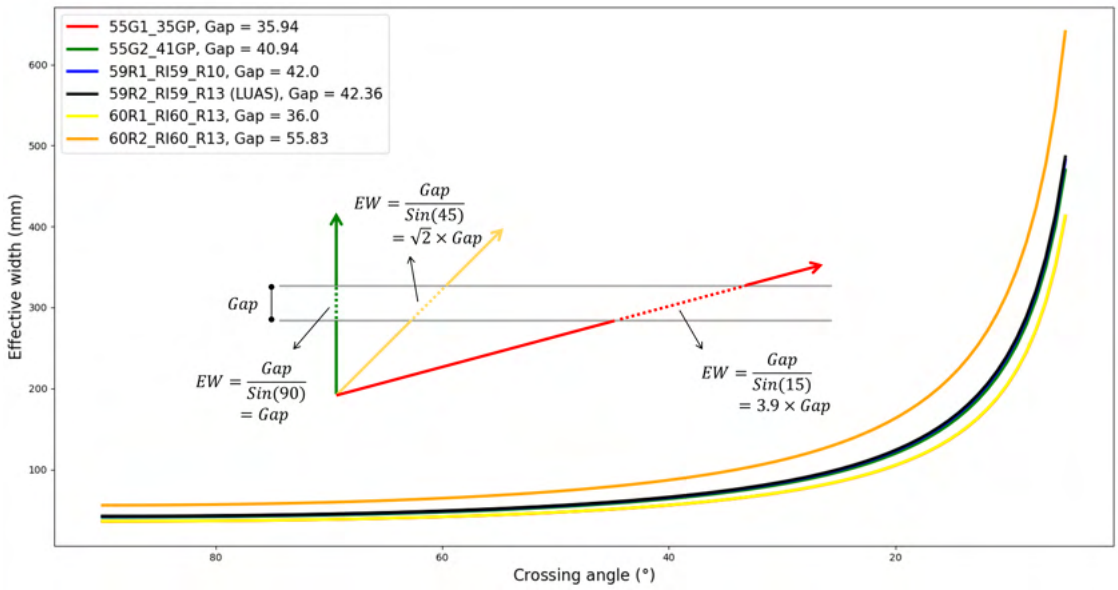

Figure 2: Effective track groove gap width (EW) by crossing angle (θ) for various track types. Some of the curves overlap.

3.3 Frequency and risk analysis

Using the collected footage, exposure and time-based risk analyses were performed to assess the rate of Unsuccessful Crossings (UCs) compared to Successful Crossings (SCs) at each recording site. UCs are here defined as falls and near-falls involving evidence of loss of control.

3.4 Fall type taxonomy

Three broad categories were defined for UCs (Figure 3).

Figure 3: The three defined categories for unsuccessful crossings (UCs).

3.5 Crossing angles and trajectories

Footage of UCs, and a random sample of SCs were extracted for analysis. T-Analyst software (developed in the European InDev project[4]) was used to calculate cyclist velocities and trajectories (Johnsson, Norén, Laureshyn, and Ivina 2018). In this framework, T-calibration allows for ground-plane calibration of monocular traffic camera footage from manually annotated scene points in both the traffic camera footage and a satellite image (with scale) of the recording location (e.g. Google Earth) (Tsai 1987) (see Figure 4). Once calibrated, 3D bounding boxes were annotated for each frame, corresponding to discrete cyclist positions over time on the X-Y plane (ground). Tracks were annotated in a similar way, using points on the ground plane. For cases involving straight tracks a cardinal axis along the track was defined during calibration, and for curved tracks pixel coordinates were annotated along the track and a 2^{nd} order polynomial was fitted in post-processing.

[4]https://cordis.europa.eu/project/id/635895/

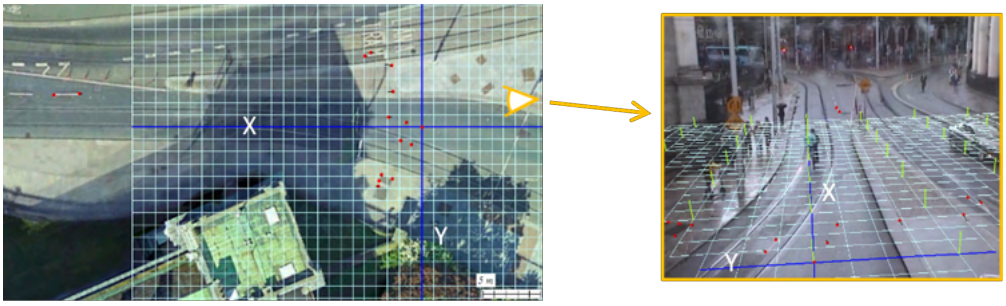

Figure 4: Ground plane calibration for Westmoreland St./College St. (Camera 7).

For calculation of crossing angles (0-90°) and velocities (m/s), a time window was defined based on visual inspection using frames before and after crossing for SCs and only frames before crossing for UCs. Crossing angles were calculated as angles between line segments representing the track and the cyclist trajectory at that location. Frame-based velocity estimates were calculated from trajectories using the central difference method and the camera framerate, and averaged across the window. Cases were excluded if the view of the cyclist was obstructed, the initial track interaction occurred out of frame, or if tracking confidence was affected by distance from the camera (image or calibration quality).

3.6 Statistical analysis and predictive modelling of crossing success

Binary logistic regression modelling was used to establish the combined effects of crossing angle and velocity on crossing success (Equation 1).

$$p = P\left(Y = 1 | X = x_1, \ldots, X_i = x_i\right) = \frac{e^{\alpha+\beta_1 x_1 \cdots + \beta_i x_i}}{1+e^{\alpha+\beta_1 x_1 \cdots + \beta_i x_i}} \quad (1)$$

where the dependent variable Y takes two values (1, 0), β_i are the coefficients estimated

using the method of maximum likelihood and x_i are the predictor variables. In modelling, a random sample of SCs across the study locations was used. To satisfy the assumption of 'independence of observations', only one crossing of one track is included for each cyclist. Both effect estimation and predictive modelling were considered, and three models were created, one for effect estimation (a) and two for predictive modelling (b & c). Model (b) was derived using crossing angle (θ) as the independent variable (IV), whereas for model (c) θ was transformed into EW (Figure 2). For effect estimation (model (a)), all variables were included, while for predictive modelling only significant variables were included (Harrell 2015). A Pearson correlation coefficient was computed to determine the relationship between IVs, indicating non-significant relationships between velocity and (1) (r(108) = -0.046, p=0.64), and (2) EW (r(108) = -0.008, p=0.936). The IVs were found to be linearly related to the logit of the dependent variable (crossing success) via the Box-Tidwell procedure, with $p > 0.05$. No outliers were found (absolute value of standardised residual greater than 2.5). Predictive models are used in the definition of a SMoS for cyclist-tram track interactions. For this purpose, Equation 2 is defined for predicting the number of UCs (N_{UC}) at a site over a period of time using a representative random sample of estimated crossing angles ($\underline{\theta} = [\theta_1, \ldots, \theta_M]$), and a count of cyclist numbers (N_C).

$$N_{UC} = N_C \times \frac{\sum_{m=1}^{M} \left\{ 1 - \frac{e^{\alpha+\beta x_m}}{1+e^{\alpha+\beta x_m}} \right\}}{M} \tag{2}$$

where α, β are taken from the modelling, and $\underline{x} = \underline{\theta}$ for model (b), or $\left[\frac{Gap}{sin(\theta_1))}, \ldots, \frac{Gap}{sin(\theta_M))} \right]$ for model (c).

3.7 Domain-specific cyclist detection

Many deep learning-based object detection algorithms exist, however, YOLO is considered the state-of-the-art for real-time object detection (Wang, Bochkovskiy, and Liao 2022). The native model has a general-purpose object detector trained on the Microsoft Common Objects in Context (MS COCO) dataset (Lin, Maire, Belongie, Hays, Perona, Ramanan, Dollar, and Zitnick 2014). However, differences in image viewpoints, qualities, and textures between MS COCO training images and domain-specific Dublin city images may result in sub-optimal performance.

For the purposes of domain transfer, a Convolutional Neural Network (CNN) which is pre-trained on a large dataset can be retrained using a comparatively small amount of data for the same task but in a different domain. The YOLO object detection model has been shown to yield successful domain-specific results after further learning on domain specific examples e.g. (Tabassum, Ullah, Al-Nur, and Shatabda 2020) [5]. The YOLOv5x model was used as a base for the task. This is the largest (166MB) and best performing YOLO model in terms of Mean Average Precision (50.7mAP$_{coco}$), i.e., the object detector predicts classes with bounding boxes, and the mAP is a single value used to score how well detections are made across all classes .

Person and bicycle classes were annotated for 259 images across the collected data [6], 233 of which were used for retraining the model, and 26 were held for validation (10% of the total). Training was performed for 50 epochs, with a batch size of 4 on an Intel® Core™ i7-9700 processor.

[5]https://github.com/ultralytics/yolov5/

[6]https://github.com/ManivannanMurugavel/Yolo-Annotation-Tool-New-/

4 Results

4.1 Data summary

Table 1 shows a summary of the collected data. A total of 2,905 cyclist interactions with tram tracks were surveyed over two periods with wet road conditions. Extracted footage includes 13 UCs (4 Cat. 1, 5 Cat. 2, and 4 Cat. 3 – see Table 4), and a random sample of the total (2,891) SCs. A total of 9 UCs were identified over Period 1 (7 hours) out of 2,741 cyclists, corresponding to an UC rate of $3.3\text{x}10^{-3}$ (approx. 3 in a 1000). A higher rate was observed in Camera 7 (Westmoreland St./College St.) (4 UCs for 213 cyclists), and a further 5 hours of footage was examined in this location (Period 2), during which a further 4 UCs were noted. Overall, this location has a UC rate of $2.1\text{x}10^{-2}$, or 21 in 1,000.

Table 1: Summary description of the study data, and UC risk estimates.

Camera	No. cyclists	Hours	UC	UC/No. cyclists	UC/Hour
1	198	7	1	0.005	0.143
2	145	7	0	0	0
3	181	7	1	0.005	0.143
4	116	7	0	0	0
5&6	410	7	1	0.002	0.143
7	377	12	8	0.021	0.667
8	324	7	1	0.003	0.143
9	551	7	1	0.002	0.143
10	603	7	0	0	0
Total	2,905	68	13	0.004	0.191

4.2 Site study: Camera 1

The majority of crossings at this location (Abbey St./Beresford St.) were at the nearside of the road at a safe crossing angle ($\overline{\theta} = 38°$) (Figure 5). The single fall at this location occurred further down

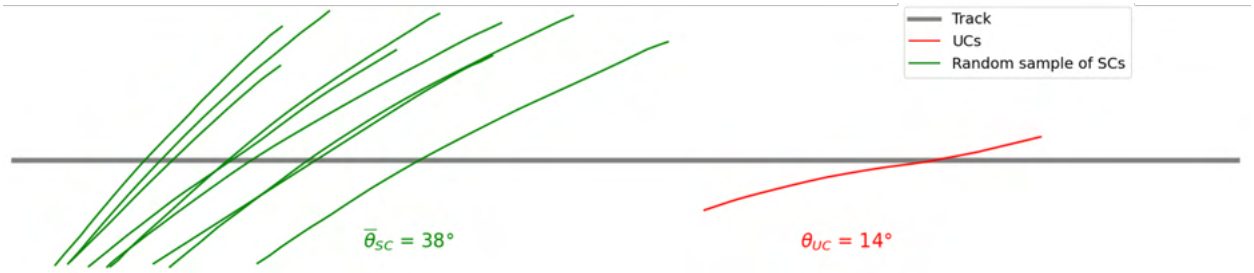

Figure 5: Trajectory analysis of cyclist interactions with a track at Abbey St./Beresford St. (Camera 1).

the tracks where the cyclist travelled more parallel to the tracks, and was passed by a motorised vehicle while crossing (θ = 14°) (Figure 6).

4.3 Site study: Camera 7

Most UCs at this location occurred on the inside track (N=7, 87%), and the analysis focused on these cases. Trajectories of 6 UCs and a random sample of 7 SCs over the inside track were annotated for Camera 7 (Figure 7). Mean crossing angles were higher for SCs ($\overline{\theta}$ = 17°, SD = 3.5), compared to UCs ($\overline{\theta}$ = 10°, SD = 5.9). The results of a Mann-Whitney U test indicate significant difference between groups (U = 8, p = 0.03). Average velocities were similar: 4.2m/s for SCs vs. 4.0m/s for UCs. Falls on the inside kerb were common, and crossing angles were low for both SCs and UCs ($\leq$ 20° - excluding one case with intentional mounting of the kerb). This is likely due to the proximity of the nearside kerb (1.16m from the track on average), which limits crossing angle.

4.4 Multivariable testing and predictive modelling for crossing success

Vectors representing the trajectories for UCs and SCs included in the modelling analysis are shown in Figure 8. Mean crossing angles and velocities (and their standard deviations) are also included.

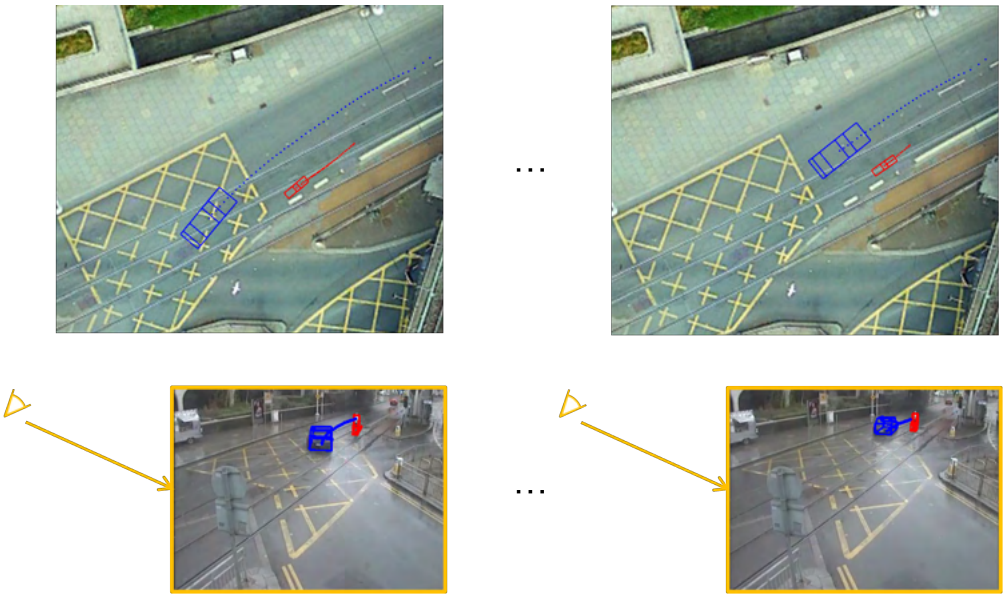

Figure 6: Cat. 3 fall at Abbey St./Beresford St. (Camera 1).

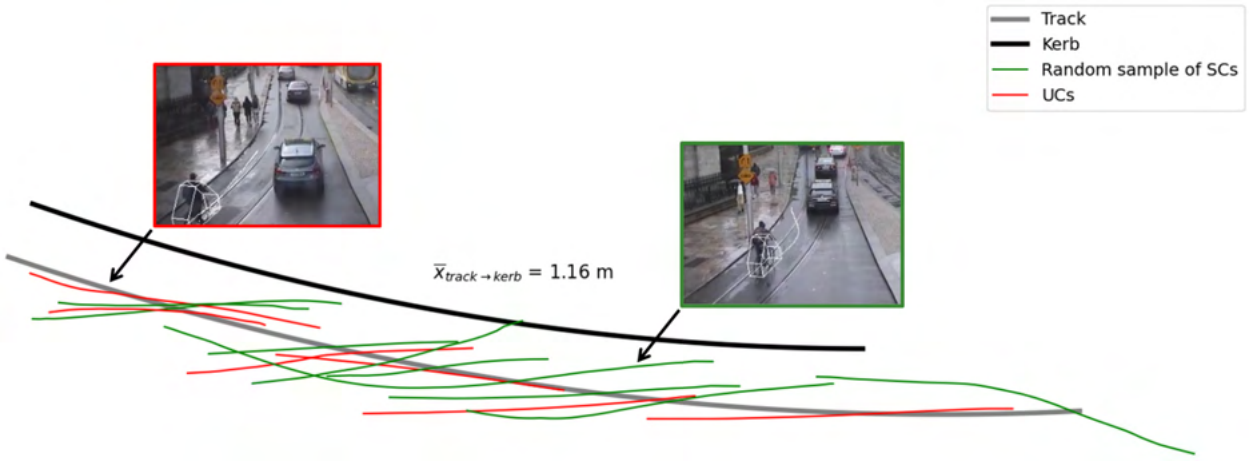

Figure 7: Trajectory analysis of cyclist interactions with the inside track at Westmoreland St./College St. (Camera 7).

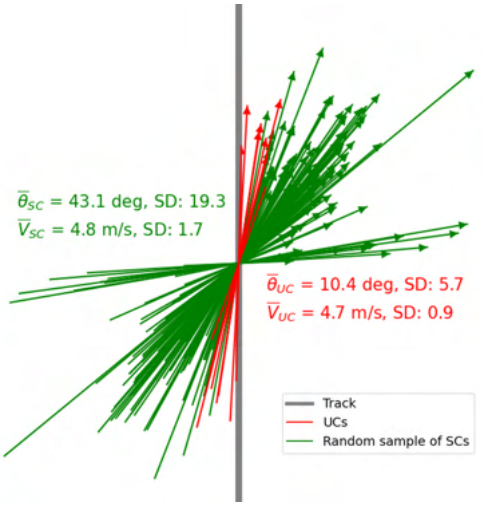

Figure 8: Crossing angles and velocities (vector magnitudes).

Mean crossing angles are notably shallower for UCs (10° vs. 43°), while mean velocities are very similar (4.7m/s vs. 4.8m/s).

4.4.1 Model (a) Effect Estimation

Binary logistic regression modelling was used to assess the combined effect of crossing angle and velocity, and to define a predictive model for crossing success. Only crossing angle was significant, see Table 5. The model was statistically significant $\chi^2(2) = 39.017$, $p < 1x10^{-8}$, Nagelkerke R^2: 74%.

4.4.2 Model (b) Predictive Modelling Using θ as the IV

Model (b) was also statistically significant, $\chi^2(1) = 37.980$, $p < 1x10^{-9}$, Nagelkerke R^2: 72% (Figure 9). It correctly classified 96% of cases, and the area under the Receiver Operating Characteristic (ROC) curve was 0.98 (95% CI: 0.956-1.000) (Figure 19), considered an outstanding level of discrimination (Hosmer, Lemeshow, and Sturdivant 2013).

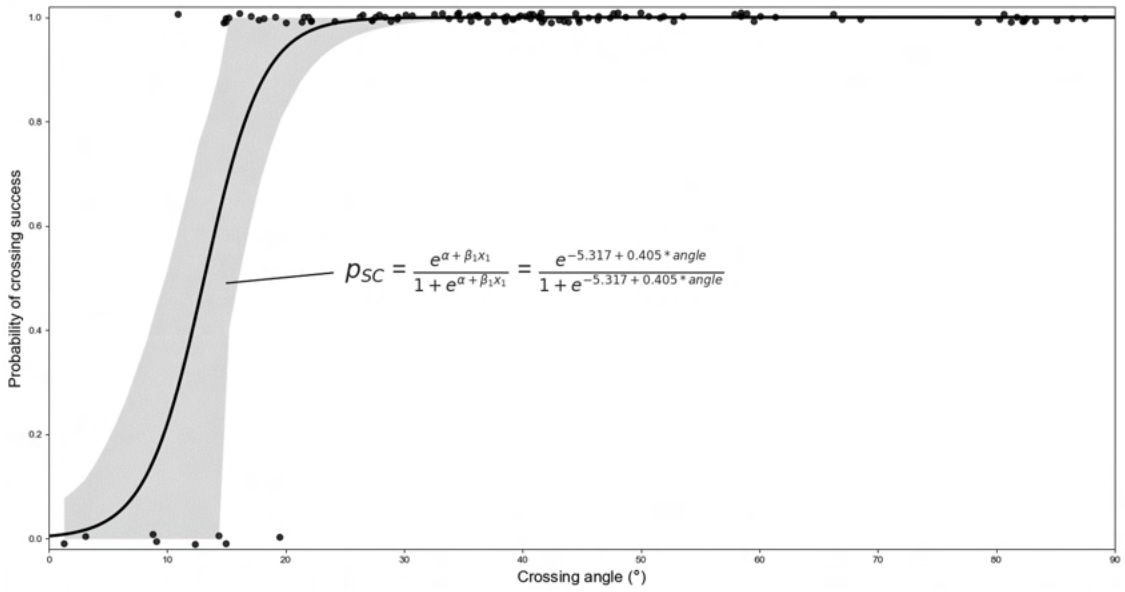

Figure 9: SC probability risk curve by crossing angle with 95% confidence levels for model (b).

SC probabilities for various crossing angles based on model (b) are shown in Figure 10. Results place the boundary for the definition of a minimum 'safe' crossing angle in the region of 25-30°. Below this, the probability of a SC decreases dramatically. Most notably, between 17.5° and 10° the probability of a SC drops from 0.85 to 0.22.

4.4.3 Model (c) Predictive Modelling Using *EW* as the IV

Model (c) was also statistically significant, $\chi^2(1) = 33.987$, $p < 1x10^{-8}$, Nagelkerke R^2: 70%, and the area under the Receiver Operating Characteristic (ROC) curve was the same as model (b) 0.98 (95% CI: 0.956-1.000). Using this, approximate risk curves can be defined for a variety of track types (Fig 11).

SC probabilities for various crossing angles based on model (c) are shown in Figure 12, showing slightly different results to model (b) (Figure 10). Although these findings also place the

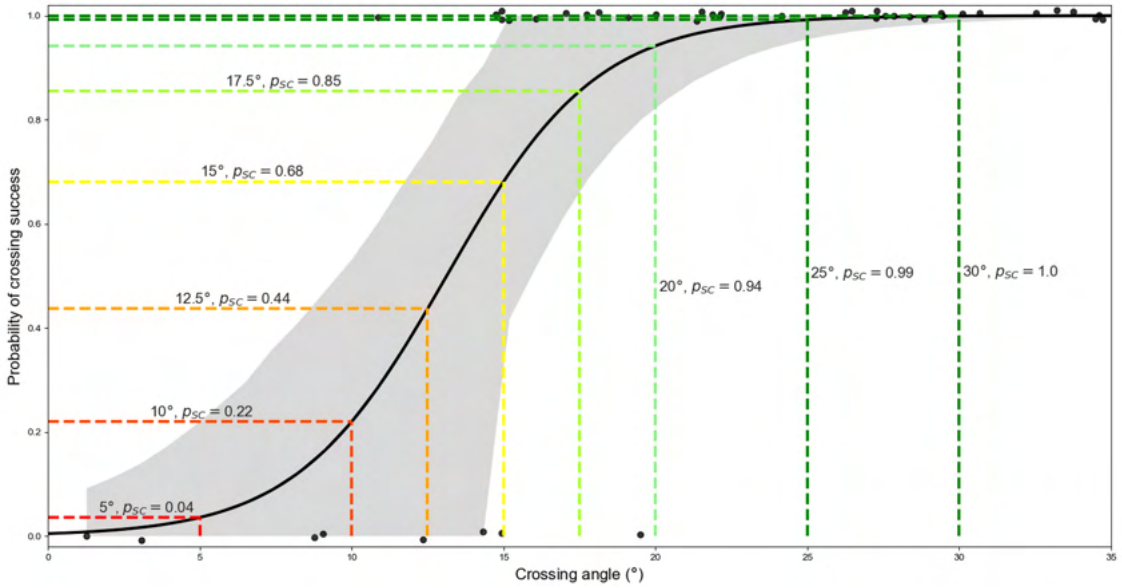

Figure 10: SC probabilities for various crossing angles from model (b).

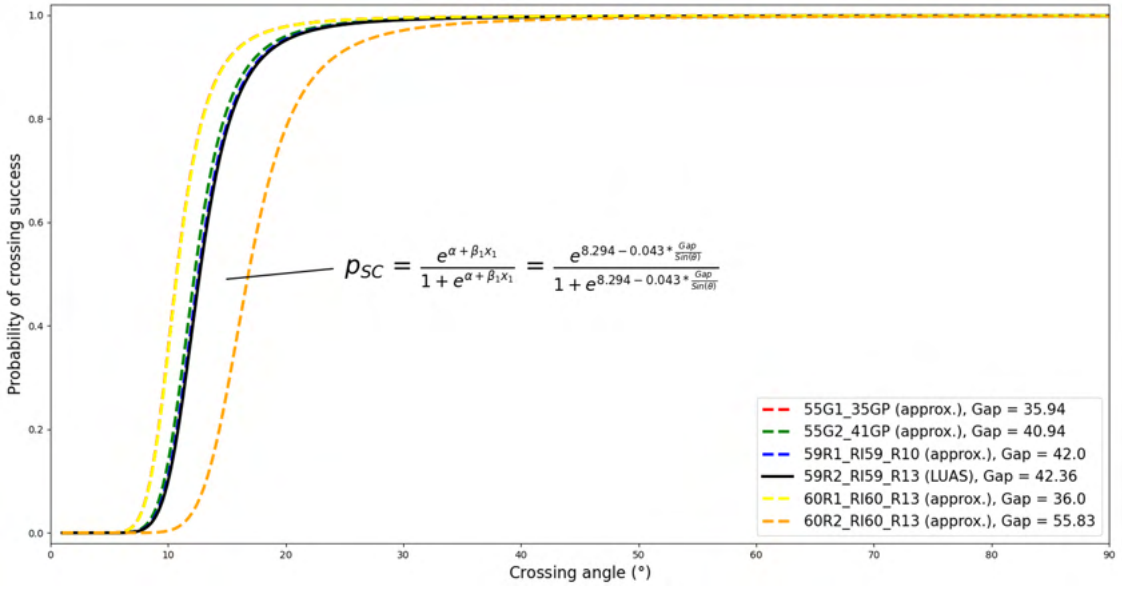

Figure 11: Approximate SC probability risk curves for various track types, vs. crossing angle, calculated as a function of effective track width from model (c).

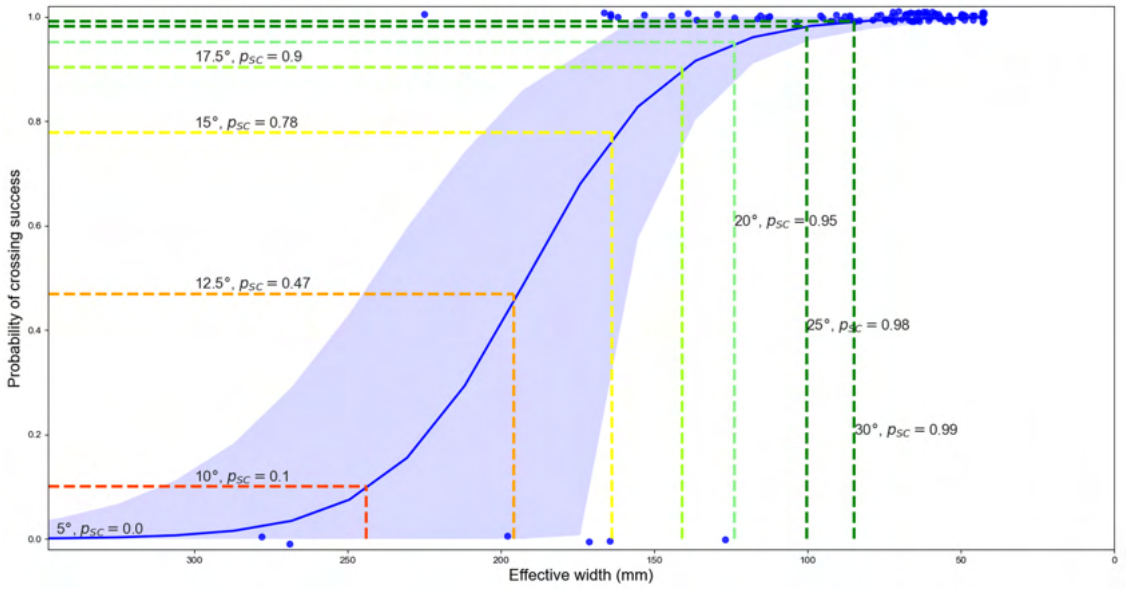

Figure 12: SC probabilities for various crossing angles from model (c) (Groove gap = 42.36mm).

boundary for minimum 'safe' crossing angles in the region of 25-30°, for lower crossing angles the associated SC probabilities drop more rapidly. For example, between 17.5° and 10° the probability of a SC drops from 0.9 to 0.1.

4.5 Application of predictive models for SMoS

Section 4.4 showed there are some differences in risk curves between predictive models (b) and (c). Table 2 shows the effect of the chosen model on the prediction of UC numbers, i.e. in the application of Equation 2. Although the models deviate somewhat for shallower crossing angles (<25°), in application they predict very similar N_{UC} levels.

Table 2: Predicted numbers of UCs for models (b) and (c), where N_C=1,000, and M=100, with randomly generated angles ($\underline{\theta}$) within a stated range.

θ **range**	**Model (b)**	**Model (c)**	**% diff**
0-10°	946	993	2%
0-20°	614	617	0%
0-30°	527	537	1%
0-40°	327	336	1%
0-50°	309	322	2%
0-60°	268	269	0%
0-70°	145	149	1%
0-80°	142	149	2%
0-90°	191	194	1%

4.6 Further training for domain-specific cyclist detection

Figure 13 shows the accuracy results for YOLOv5x after further training on domain-specific Dublin city images.

Figure 14 shows a qualitative comparison of inference accuracy between the native YOLOv5x, and the retrained model YOLOv5xDCC (confidence threshold=0.6) for cases in the test set. Further results on videos are available[7].

4.7 Automatic vs. manual tracking

Inference was performed using model YOLOv5xDCC for a sample of 5 SCs, and 1 UC at camera 1 to compare estimated crossing angles between manual and automatic approaches. A point at the lower end of the bounding box ($y = 0.25h$, $x = 0.5w$) was used for the ground position in each frame, and a Savitzky-Golay filter was used for smoothing. Crossing angles were broadly similar; the automatic tracking yielded an average of 36°, compared to 37° for manual tracking (see Table 3, and Figure 15).

[7]https://github.com/KevGildea/SafeCross/tree/main/YOLOv5xDCC/Examples/

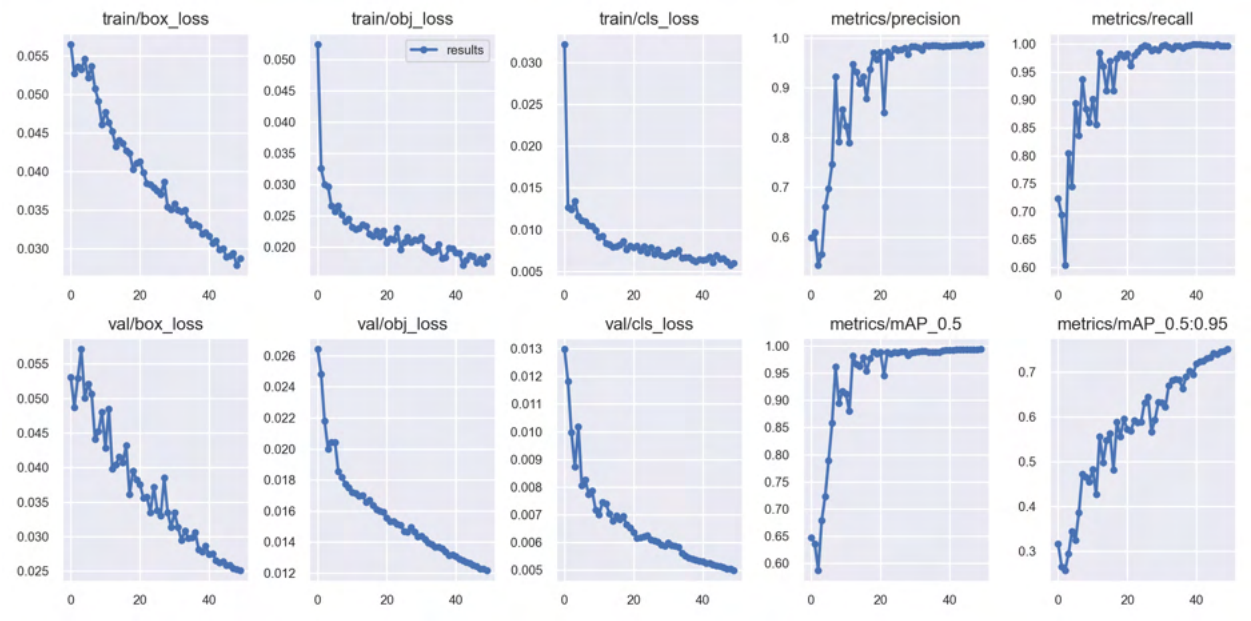

Figure 13: Accuracy results for YOLOv5x after further training on domain-specific Dublin city images.

5 Discussion

High overall incidence of UCs was observed over this short study period with limited coverage of the track network, highlighting the significance of the safety issue. These findings support results from a self-reporting collision survey (Gildea, Hall, and Simms 2021). One location had a particularly high risk (Camera 7: Westmoreland St./College St), and an additional UC was noted for an adjacent study location (Cameras 5&6: College Green). Overall UC rates were approx. 21/1000 cyclists at Camera 7, vs. approx. 3/1000 overall. These findings are similar to a study in the US for railway tracks, which found fall rates of 2/1000 at one location, and 15/1000 at another (Ling, Cherry, and Dhakal 2017), from a sample including over 13,000 cyclist traversings over a 2 month period. By comparison, the sample in this study was over only 7 hours over 8 locations around the city (plus an

Figure 14: Visualisation of model improvements between YOLOv5x and YOLOv5xDCC for a sample of images.

added 5 hours for camera 7).

At Camera 7: Westmoreland St./College St, the majority of UCs (N=7, 87%) occurred on the inside/nearside track where a kerb runs alongside in close proximity (see Figure 7). UCs at this location are likely due to the proximity of this kerb. All crossings in this location (including both UCs and SCs) are far below the mean crossing angle seen across other locations. For SCs, crossing angles at this location were an average of 17° vs. 43° overall. Extending the roadway at this location to allow for safe crossing angles would likely have a significant impact on the fall rates. The authors recommend physical separation of cyclists from tram tracks, and at locations where cyclists are expected to cross tracks, sufficient space should be available for a safe approach angle. Furthermore,

Case	Manual	Automatic
SC 1	44°	43°
SC 2	33°	34°
SC 3	41°	38°
SC 4	36°	35°
SC 5	32°	31°
UC 1	14°	15°

Table 3: Comparison of crossing trajectories for a sample of cases at camera 1.

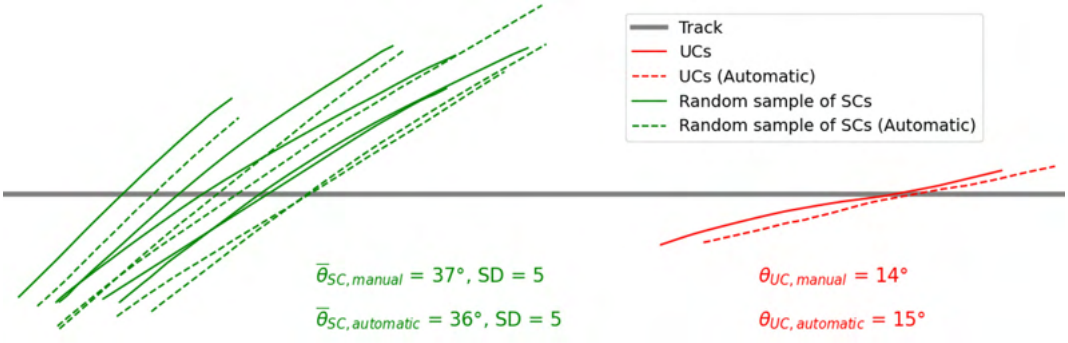

Figure 15: Comparison of crossing trajectories for a sample of cases at camera 1.

by visual inspection, most (N=12, 92%) UCs at other locations involve obstacles that limit crossing angle, i.e. kerbs or nearby/passing vehicles/other cyclists (Table 4). The Safe System approach calls for prioritisation of system level redesign over attempts to influence individual behaviour (ITF 2016), therefore, the authors recommend engineering interventions be prioritised to allow for safe crossing angles. Furthermore, since many cases involve a passing/nearby motorised vehicles (N=4, 31%), the authors recommend efforts to increase priority for cyclists at crossings, and provision of segregated lanes where possible. Indeed, international literature indicates that traffic pressure contributes to the majority of falls on tram tracks (Maempel, Mackenzie, Stirling, McCann, Oliver, and White 2018).

Descriptive statistics (Figure 8) show that while mean crossing velocities are similar across SCs and UCs (4.8m/s vs. 4.7m/s), mean crossing angles were not (43° vs. 10°). Therefore, as

expected, from multivariable modelling, crossing angle was found to be a strong predictor of crossing success. Though crossing velocity was not a significant predictor (Table 5), similar to (Ling, Cherry, and Dhakal 2017), it is possible that velocity could factor into a multiclass predictive model. With this in mind, a multinomial regression was performed with crossing categories, i.e., a dependent variable with 4 levels (SC, UC-Cat. 1, UC-Cat. 2, UC-Cat. 3), however, the model was not statistically significant and had low discrimination. With a greater sample size, such a model may reveal predictive effects. As described in section 4.4, of the two predictive models (b & c), there are slight differences in risk curves. Specifically, while both models indicate that the boundary for the definition of a minimum 'safe' crossing angle in the region of 30°, SC probabilities vary below this. These differences are tested in the context of a potential SMoS for prediction of UC numbers (N_{UC}) in section 4.5, showing that both models predict similar numbers in application, though model (c) generally predicts slightly higher numbers. Furthermore, model (c) allows for approximate risk estimates for crossings on tracks with different groove gap widths, which may be useful for other locations with different track types.

Infrastructural planners in Dublin/Ireland should plan for road designs that allow for and encourage crossing angles of 30° or more. However, for site-specific infrastructural planning it may be difficult to account for all common cyclist trajectories, highlighting the potential utility of this SMoS framework.

Proof-of-concept is provided that further training on a relatively small sample of domain specific data can achieve substantial accuracy improvements for cyclist detection in traffic camera footage. The accuracy of the native YOLOv5x model applied to DCC data was 0.65mAP$_{0.5}$, i.e., with an Intersection over Union (IoU) threshold of 0.5, after training this rose dramatically to 0.99mAP (Figure 13). Averaging mAP for IoU thresholds between 0.5 and 0.95 (as per (Huang, Rathod, Sun, Zhu, Korattikara, Fathi, Fischer, Wojna, Song, Guadarrama, and Murphy 2017)) showed similar

improvements, from 0.32mAP$_{0.5:0.95}$ to 0.75 mAP$_{0.5:0.95}$. Qualitatively, these improvements are also observed between the models (Figure 13). Furthermore, in application, automatically inferring trajectories using the YOLOv5xDCC model yields very similar crossing angles to manual tracking. Future work will incorporate automatic cyclist trajectory detection into the SafeCross application, which after after ground-plane calibration, i.e., T-Calibrate (Johnsson, Norén, Laureshyn, and Ivina 2018), may allow for semi-automatic prediction of unsuccessful crossings (see Figure 17).

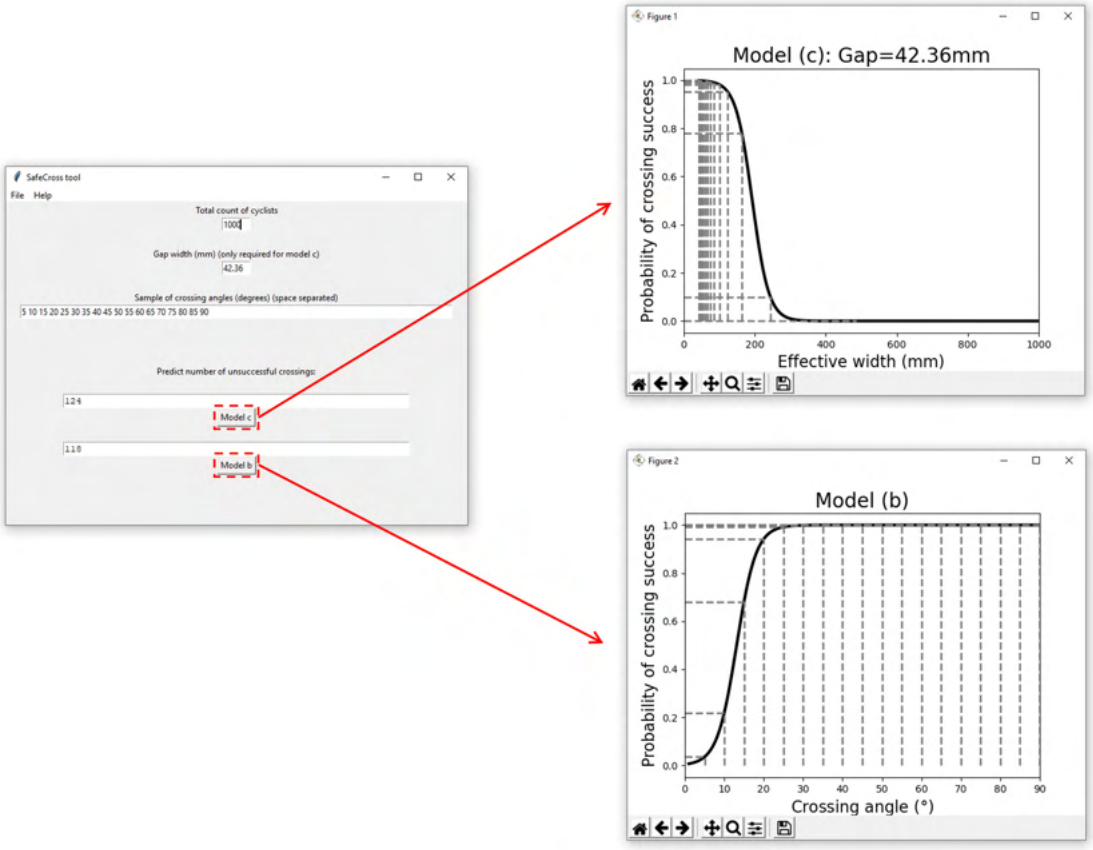

Figure 16: SafeCross tool.

6 Conclusions

This study presents the first video-based trajectory and fall analysis for cyclist interactions with light rail tram-tracks. The analysis focuses on wet road conditions as a common and safety-critical edge case. Actionable site-specific safety issues at locations in Dublin city centre are highlighted, and the risk of UC occurrence by crossing angle is modelled. As evident by the prevalence of external factors limiting crossing angle (e.g. kerbs, other road users), personal responsibility/educational campaigns targeted towards cyclists are unlikely to address the majority of falls on tracks. In the context of the Safe System approach, i.e., to proactively target and treat risk, these findings imply the need for bolstered data collection regimes in urban environments, and engineering interventions to facilitate safe crossing angles. The use of the validated SMoS algorithm developed in this study can help achieve these goals, and an open-source application is provided for this purpose (SafeCross[8]) (see Figure 16).

[8]https://kevgildea.github.io/SafeCross/

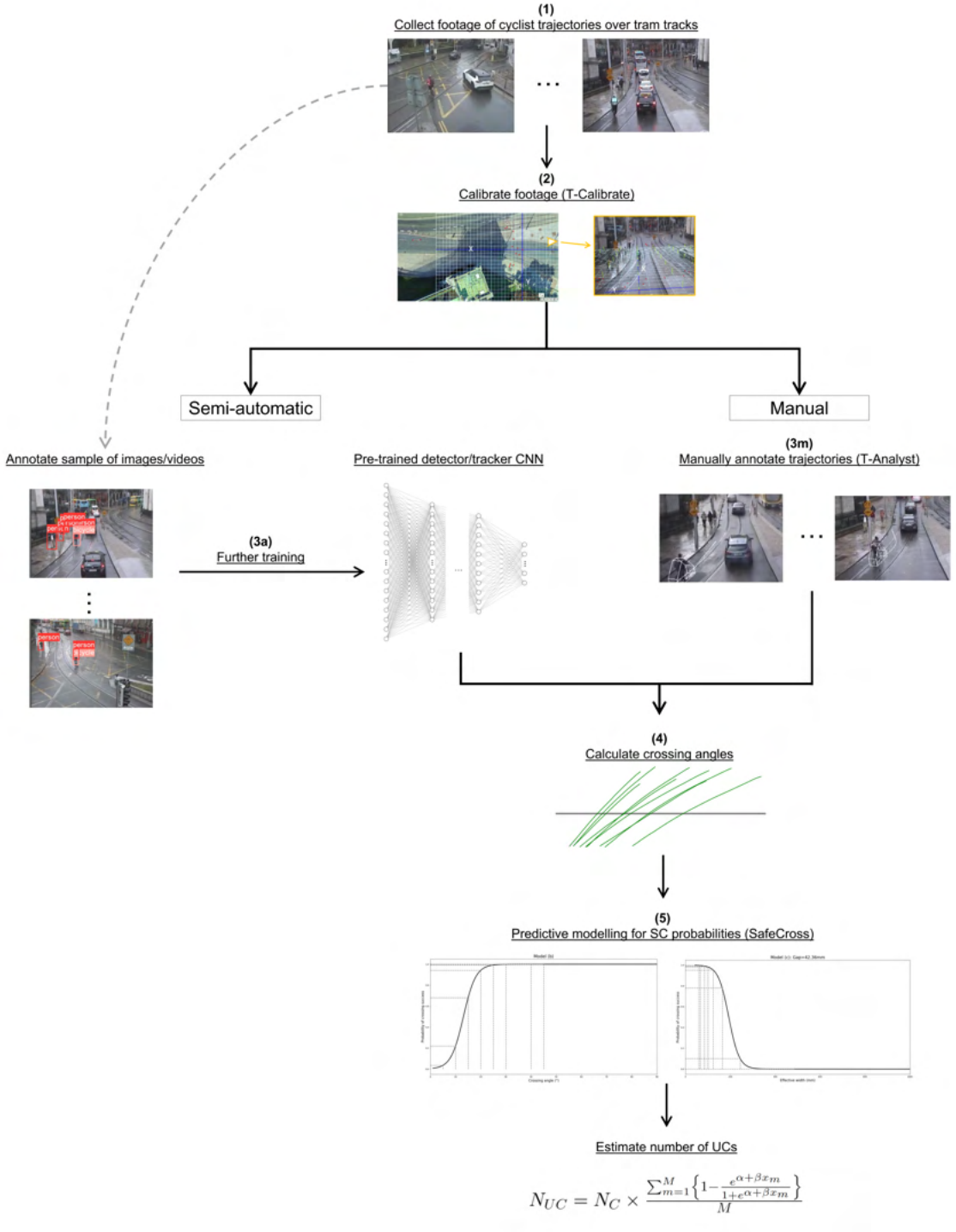

Figure 17: Proposed pipeline for prediction of UCs on tram tracks.

References

Allen, Brian, Tom Shin, and Peter Cooper. 1978. "Analysis of traffic conflicts and collisions." *Transportation Research Record* 667:67–74.

Beck, Ben, Mark R. Stevenson, Peter Cameron, Jennie Oxley, Stuart Newstead, Jake Olivier, Soufiane Boufous, and Belinda J. Gabbe. 2019. "Crash characteristics of on-road single-bicycle crashes: An under-recognised problem." *Injury Prevention* .

Bornø Jensen, Morten, Martin Ahrnbom, Maarten Kruithof, Karl Åström, Mikael Nilsson, Håkan Ardö, Aliaksei Laureshyn, Carl Johnsson, and Thomas Moeslund. 2019. "A Framework for Automated Traffic Safety Analysis from Video Using Modern Computer Vision." In *Transportation Research Board Annual Meeting 2019*.

Gildea, Kevin, Daniel Hall, and Ciaran Simms. 2021. "Configurations of underreported cyclist-motorised vehicle and single cyclist collisions: Analysis of a self-reported survey." *Accident Analysis Prevention* 159:106264.

Gildea, Kevin and Ciaran Simms. 2021. "Characteristics of cyclist collisions in Ireland: Analysis of a self-reported survey." *Accident Analysis Prevention* 151:105948.

Harrell, Frank E. 2015. *Regression Modeling Strategies*. Springer Series in Statistics. Springer International Publishing.

Hayward, J. 1971. *Near Misses as a Measure of Safety at Urban Intersections - John Charles Hayward*. Ph.D. thesis, Pennsylvania State, USA.

Hertach, Patrizia, Andrea Uhr, Steffen Niemann, and Mario Cavegn. 2018. "Characteristics of single-vehicle crashes with e-bikes in Switzerland." *Accident Analysis Prevention* 117:232–238.

Hosmer, David W., Stanley. Lemeshow, and Rodney X. Sturdivant. 2013. *Applied logistic regression.*

Huang, Jonathan, Vivek Rathod, Chen Sun, Menglong Zhu, Anoop Korattikara, Alireza Fathi, Ian Fischer, Zbigniew Wojna, Yang Song, Sergio Guadarrama, and Kevin Murphy. 2017. "Speed/accuracy trade-offs for modern convolutional object detectors." *Proceedings - 30th IEEE Conference on Computer Vision and Pattern Recognition, CVPR 2017* 2017-January:3296–3305.

ITF. 2016. "Zero Road Deaths and Serious Injuries Leading a Paradigm Shift to a Safe System." Technical report, OECD.

Johnson, Marilyn, Judith Charlton, Jennifer Oxley, and Stuart Newstead. 2010. "Naturalistic Cycling Study: Identifying Risk Factors for On-Road Commuter Cyclists." *Annals of Advances in Automotive Medicine / Annual Scientific Conference* 54:275.

Johnsson, Carl, Hampus Norén, Aliaksei Laureshyn, and Daria Ivina. 2018. "InDev Deliverable 6.1: T-Analyst - semi-automated tool for traffic conflict analysis." Technical report.

Laureshyn, Aliaksei, Maartje de Goede, Nicolas Saunier, and Aslak Fyhri. 2017. "Cross-comparison of three surrogate safety methods to diagnose cyclist safety problems at intersections in Norway." *Accident Analysis and Prevention* 105:11–20.

Lin, Tsung-Yi, Michael Maire, Serge Belongie, James Hays, Pietro Perona, Deva Ramanan, Piotr Dollar, and Larry Zitnick. 2014. "Microsoft COCO: Common Objects in Context." In *ECCV*. European Conference on Computer Vision.

Ling, Ziwen, Christopher R. Cherry, and Nirbesh Dhakal. 2017. "Factors influencing single-bicycle crashes at skewed railroad grade crossings." *Journal of Transport Health* 7:54–63.

Maempel, J. F., S. P. Mackenzie, P. H. C. Stirling, C. McCann, C. W. Oliver, and T. O. White. 2018. "Tram system related cycling injuries." *Archives of Orthopaedic and Trauma Surgery* pp. 1–8.

Schepers, P., B. de Geus, J. van Cauwenberg, T. Ampe, and C. Engbers. 2020. "The perception of bicycle crashes with and without motor vehicles: Which crash types do older and middle-aged cyclists fear most?" *Transportation Research Part F: Traffic Psychology and Behaviour* 71:157–167.

Shinar, D., P. Valero-Mora, M. van Strijp-Houtenbos, N. Haworth, A. Schramm, Guido De Bruyne, V. Cavallo, J. Chliaoutakis, J. Dias, O.E. Ferraro, A. Fyhri, A. Hursa Sajatovic, K. Kuklane, R. Ledesma, O. Mascarell, A. Morandi, M. Muser, D. Otte, M. Papadakaki, J. Sanmartín, D. Dulf, M. Saplioglu, and G. Tzamalouka. 2018. "Under-reporting bicycle accidents to police in the COST TU1101 international survey: Cross-country comparisons and associated factors." *Accident Analysis Prevention* 110:177–186.

Skelton, Dick. 2016. "Tram/Cycle infrastructure Review Study." Technical report, Sheffield City Council.

Strauss, Jillian, Sohail Zangenehpour, Luis F. Miranda-Moreno, and Nicolas Saunier. 2017. "Cyclist deceleration rate as surrogate safety measure in Montreal using smartphone GPS data." *Accident Analysis Prevention* 99:287–296.

Tabassum, Shaira, Md Sabbir Ullah, Nakib Hossain Al-Nur, and Swakkhar Shatabda. 2020. "Native Vehicles Classification on Bangladeshi Roads Using CNN with Transfer Learning." *2020 IEEE Region 10 Symposium, TENSYMP 2020* pp. 40–43.

Tsai, Roger Y. 1987. "A Versatile Camera Calibration Technique for High-Accuracy 3D Machine Vision Metrology Using Off-the-Shelf TV Cameras and Lenses." *IEEE Journal on Robotics and Automation* 3:323–344.

UITP. 2019. "Light rail and tram: The European outlook." Technical report.

Wang, Chien-Yao, Alexey Bochkovskiy, and Hong-Yuan Mark Liao. 2022. “YOLOv7: Trainable bag-of-freebies sets new state-of-the-art for real-time object detectors.” .

Appendices

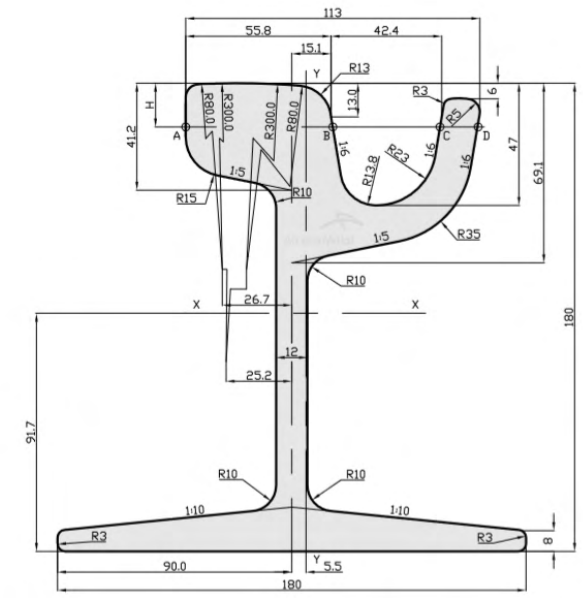

Figure 18: Profile of the 59R2 (Ri59N) grooved rail.

Table 4: All UCs noted in this study.

Case 1 • Camera 1 • Cat 3.	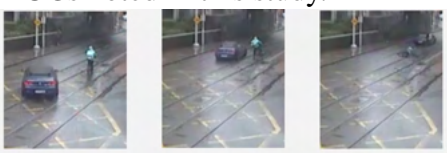
Case 2 • Camera 3 • Cat 2.	
Case 3 • Camera 5 • Cat 2.	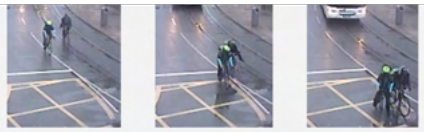
Case 4 • Camera 7 • Cat 2.	
Case 5 • Camera 7 • Cat 2.	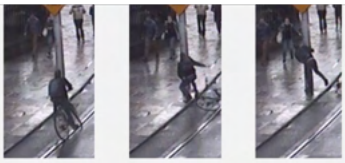
Case 6 • Camera 7 • Cat 3.	
Case 7 • Camera 7 • Cat 1.	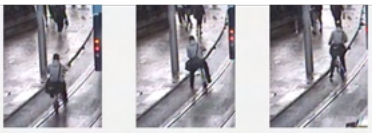
Case 8 • Camera 7 • Cat 1.	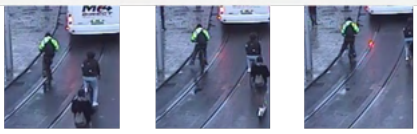

Cont...

Case 9

- Camera 7
- Cat 3.

Case 10

- Camera 7
- Cat 1.

Case 11

- Camera 7
- Cat 2.

Case 12

- Camera 8
- Cat 3.

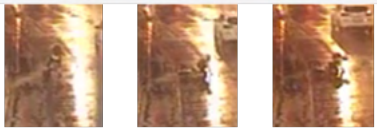

Case 13

- Camera 9
- Cat 1.

Table 5: Results for regression model (a).

							95% C.I.for Exp(β)	
	β	S.E	Wald	df	Sig.	Exp(β)	Lower	Upper
Crossing angle	.489	.215	5.152	1	.023	1.630	1.069	2.486
Velocity	.671	.745	.812	1	.368	1.957	.454	8.431
Constant	-9.621	5.804	2.748	1	.097	.000		

Table 6: Results for regression model (b).

							95% C.I.for Exp(β)	
	β	S.E	Wald	df	Sig.	Exp(β)	Lower	Upper
Crossing angle	.405	.161	6.328	1	.012	1.500	1.094	2.057
Constant	-5.317	2.478	4.605	1	.032	.005		

Table 7: Results for regression model (c).

							95% C.I.for Exp(β)	
	β	S.E	Wald	df	Sig.	Exp(β)	Lower	Upper
EW	-.043	.014	9.949	1	.002	.958	.932	.984
Constant	8.294	2.170	14.608	1	.000132	4000.460198		

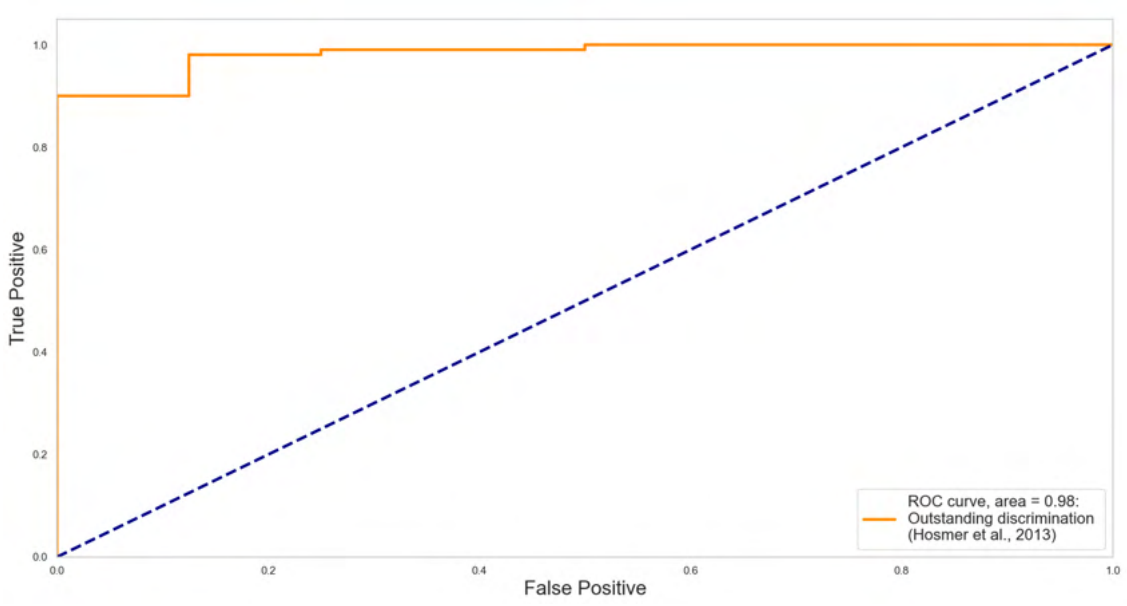

Figure 19: Receiver Operating Characteristic (ROC) curve for model (b).

CRediT authorship contribution statement

Kevin Gildea: Conceptualisation, Data curation, Formal analysis, Software, Investigation, Methodology, Resources, Validation, Visualisation, Writing - original draft, Writing - review editing, Project administration. **Daniel Hall**: Visualisation, Writing - review editing. **Clara Mercadal-Baudart**: Conceptualisation. **Brian Caulfield**: Resources, Writing - review editing. **Ciaran Simms**: Supervision, Conceptualisation, Funding acquisition, Methodology, Project administration, Resources, Writing - review editing.